

## Articles

# Resveratrol Oligomers Trans-gnetin H Promotes Reactive Oxygen Species Generation and Rictor Degradation to Suppress Cancer Cell Viability

Shiyang Lou<sup>a,1</sup>, Ruixu Zhang<sup>a,1</sup>, Chao Xia<sup>a,1</sup>, Yining Zheng<sup>a</sup>, MiaoMiao Zhu<sup>a</sup>, Dingping Feng<sup>a</sup>, Lu Deng<sup>a,b\*</sup>

DOI:<https://dx.doi.org/10.71373/UGHK9221>  
Submitted 27 June 2025  
Accepted 12 August 2025  
Published 26 August 2025



The function of resveratrol as an antioxidant is to scavenge reactive oxygen species (ROS) in the body. The effects of resveratrol on cellular activity have been widely reported. Trans-gnetin H is a trimer of resveratrol that is found in seeds of peonies. However, there is not enough research on the cellular effects of trans-gnetin H, and it is not clear if it has the same physiological functions as resveratrol. This study tries to answer this question by investigating the effect of trans-gnetin H on ROS, mammalian target of rapamycin (*mTOR*), cell viability, autophagy, and ferroptosis in several cancer cell lines. Trans-gnetin H was found to regulate cell viability, cell proliferation, and autophagy, but it did not affect ferroptosis. Molecular experiments showed that these effects were brought about via significant promotion of ROS generation and suppression of *mTOR* activation in an ROS-dependent manner. Further mechanistic experiments showed that trans-gnetin H inhibits *mTOR* activation by inducing *FBXW7*-mediated ubiquitination and degradation of *Rictor*, a key component of *mTORC2*. Thus, trans-gnetin H appears to control tumor cell viability by inhibiting activation of the *mTORC1* and *mTORC2* pathways through a novel regulatory mechanism involving the ROS-Rictor signaling axis.

## Introduction

Reactive oxygen species (ROS) are commonly found in the form of molecular oxygen derivatives such as  $O_2^-$  and  $H_2O_2$ . There are many sources of intracellular ROS, which can be generated in the plasma membrane, cytoplasm, and organelles (including the endoplasmic reticulum, mitochondria, and peroxisomes)<sup>[1]</sup>. ROS production and ROS elimination need to be balanced for the maintenance of the intracellular redox state and several cell-, organ-, and organism-level physiological processes such as formation of the extracellular matrix, wound healing, and immunity<sup>[2-4]</sup>. ROS accumulation can lead to various diseases, including cancer, by inducing oxidative damage to proteins, DNA, and lipids. Interestingly, excessive ROS levels may also cause tumor cell death. Therefore, the target of numerous chemotherapeutic methods for the treatment of tumors is ROS-induced cell death. As a result, there is considerable ongoing research about the mechanisms associated with ROS-induced cell death and related treatment targets that could be applied in cancer therapy.

Resveratrol is a commonly found polyphenolic compound with known antioxidant, anti-inflammatory, and immunomodulatory properties, among other benefits. Resveratrol has a broad spectrum of anti-tumor effects, showing significant anti-tumor activity in a variety of tumor cells. It can inhibit the growth, proliferation, invasion and metastasis of cancer cells through a variety of signaling pathways and regulate the expression of related proteins, induce cell apoptosis, and reverse chemotherapy resistance and enhance chemotherapy sensitivity. Trans-

gnetin H<sup>[5]</sup> is a natural polyphenolic compound that is structurally composed of a trimer of resveratrol and one of the most important stilbenes in peony seeds. There is a large body of literature on the antitumor effects and mechanisms of resveratrol, but studies on the antitumor activity and mechanisms of trans-gnetin H are few. In our previous study, we reported the antitumor potential of trans-gnetin H<sup>[6]</sup> and found that trans-gnetin H controls tumor cell growth through regulation of autophagy<sup>[5]</sup>. In line with this observation, it is known that resveratrol, the compound that forms trans-gnetin H, plays a role in the initiation of autophagy<sup>[7-9]</sup>. In addition, the antioxidant activity of resveratrol is one of its main functions<sup>[10-13]</sup>, and it is also known to be involved in the induction of apoptosis<sup>[9,14,15]</sup> and cell necrosis<sup>[16]</sup>. In contrast to these findings for resveratrol, the results of our previous study indicated that trans-gnetin H did not play a role in regulating apoptosis<sup>[5]</sup>. Further, it is not clear whether trans-gnetin H has antioxidant capacity. Thus, although trans-gnetin H is composed of resveratrol, it does not possess all the characteristics of resveratrol.

In our previous study, we also discovered that trans-gnetin H regulates autophagy via the mammalian target of rapamycin (*mTOR*) complex 1 (*mTORC1*) pathway. *mTOR* is an atypical serine/threonine protein kinase that integrates a variety of extracellular signals, including amino acids, glucose, lipids, growth factors, and ROS, and is essential for autophagy<sup>[17]</sup>. It is primarily found in two intracellular complexes—*mTORC1* and *mTORC2*—which are sensitive and respond to different signals (including ROS) and, thus, exert different functions<sup>[18]</sup>. In our previous study, even though we discovered that trans-gnetin H can regulate the *mTORC1* pathway, it was unclear whether it affects the *mTORC2* pathway. In the present study, we have tried to gain a better understanding of the antitumor activity and mechanisms of trans-gnetin H by investigating its effects on ROS levels and the *mTOR* pathway in several cancer cell lines. We believe that these findings will shed light on the functions of trans-gnetin H and the underlying autophagy-related mecha-

<sup>a</sup> College of Animal Science and Technology, Northwest A&F University, Yangling, Shanxi 712100, China; <sup>b</sup> Shenzhen Research Institute, Northwest A&F University, Shenzhen, Guangdong, 518000, China;

<sup>1</sup> These authors contributed equally to this article;

\* Corresponding author

denglu128128@nwafu.edu.cn (L. Deng)

Running title: Trans-gnetin H Suppress Cancer Cell Viability

nisms in tumor cells and also help identify potential therapeutic targets for antitumor treatment.

## Materials and methods

### Materials

During the design of the AMR bacteria database, we strictly *Erastin* (E7781), *RSL3* (SML2234), *cycloheximide* (*CHX*), *N-acetylcysteine* (*NAC*, A7250), *dichlorofluorescein diacetate* (*DCFH-DA*, 35845), and secondary antibodies were obtained from Sigma-Aldrich (MO, USA). Antibodies for pT389-S6K (9234S/L), S6K (9202S), *Rictor* (9476), pS473-AKT (9271), AKT (9272), and *SOD1* (37385) were obtained from Cell Signaling Technology (MA, USA). Actin (20536-1-AP), *FBXW7a* (28424-1-AP), *Nrf2* (16396-1-AP), and *HMOX1* (10701-1-AP) were obtained from Proteintech (Chicago, USA). *NQO1* (ab80588) was obtained from Abcam (Cambridge, UK).  $\beta$ -mercaptoethanol, penicillin, fetal bovine serum (FBS) and streptomycin were purchased from Gibco (Grand Island, NY, USA). Phosphate-buffered saline (PBS) and trypsin were purchased from HyClone (UT, USA). Trizol reagent, the PrimeScript RT reagent kit (RR047A), and the TB Green quantitative real-time quantitative polymerase chain reaction (*qRT-PCR*) kit (RR820A) were purchased from Takara (Dalian, China). Cell counting kit-8 (CCK8, K009) was purchased from ZETA LIFE (CA, USA). *BODIPY 581/591 C11* (D3861) was purchased from Thermo Fisher Scientific (MA, USA).

### Origin and purity of trans-gnetin H

Trans-gnetin H (purity, >99%) was obtained from the seeds of the tree peony. For the cellular experiments, trans-gnetin H was dissolved in dimethyl sulfoxide to the required concentrations. The extraction and isolation of trans-gnetin H was conducted according to the published protocol<sup>[19]</sup>. Structural determination of isolated trans-gnetin H was elucidated by *1H*- and *13C-NMR* as below:

*1H-NMR* (500 MHz, CD3OD) $\delta$  (ppm): 7.19 [4H, dd, *J* = 2.0, 8.5 Hz, H-2(6), 2" (6")], 6.79 [4H, dd, *J* = 2.0, 8.5 Hz, H-3(5), 3" (5")], 6.69 (2H, d, *J* = 8.5 Hz, H-2', 6'), 6.51 (2H, d, *J* = 8.5 Hz, H-3', 5'), 6.43 (1H, s, *J* = 8.5 Hz, H-12), 6.39 (2H, s, H-7', 8'), 6.15 [6H, s, H-10(10"), 12(12"), 14(14")], 5.41 (2H, d, *J* = 5.5 Hz, H-7, 7"), 4.41 (2H, d, *J* = 5.5 Hz, H-8, 8").

*13C-NMR* (125 MHz, CD3OD) $\delta$  (ppm): 163.5 (C-11', 13'), 160.6 [C-11(11")], 13(13")], 159.0 (C-4, 4"), 158.8 (C-4'), 148.0 (C-9, 9"), 135.0 (C-9'), 134.6 (C-1"), 134.2 (C-1), 131.1 (C-1'), 129.14 (C-2', 6', 8'), 128.6 [C-2(2")], 6(6")], 123.0 (C-7'), 120.8 (C-10', 14'), 116.8 [C-3(3")], 5(5")], 116.6 (C-3', 5'), 107.8 [C-10(10"), 14(14")], 102.6 (C-12, 12"), 95.3 (C-7, 7"), 91.9 (C-12'), 59.4 (C-8, 8").

The *1H*- and *13C-NMR* of trans-gnetin H only used for review because our related work haven't been published.

The purity of trans-gnetin H was confirmed using *HPLC*. Evidence is presented in the supplementary material of our previously published articles.

### Cell culture

HT29, H1299, MDA231, and HepG2 cells were purchased from National Science & Technology Infrastructure (NSTI, Shanghai, China) and cultured according to the manufacturer's protocol.

HT29 and H1299 cells were cultured in RPMI 1640 medium (Hyclone, USA), MDA231 and HepG2 cells were cultured in Dulbecco's modified Eagle medium (DMEM; Hyclone, USA) containing 10% FBS (Gibco, Grand Island, NY, USA) according to the ATCC guidelines.

### Sample collection and preparation for lipidomic analysis

HT29 cells were treated with 10  $\mu$ M trans-gnetin H for 2 hours. Cells from both control and trans-gnetin H-treated groups were then harvested. Six replicate samples per group (each contains 1  $\times$  10<sup>7</sup> cells precisely counted via Cytometer, BioRad, Hercules, USA) were flash-frozen in liquid nitrogen and stored at -80°C for lipid extraction and *LC-MS* analysis. Lipids were extracted following Matyash<sup>[20]</sup> with modifications. Briefly, samples were thawed at 4°C before adding 200  $\mu$ L ice-cold distilled water. Homogenization was performed with 240  $\mu$ L ice-cold methanol, followed by vortexing. After adding 800  $\mu$ L methyl tert-butyl ether (MTBE), samples were vortexed, sonicated in an ice-water bath for 20 min, then incubated at room temperature for 30 min. Following centrifugation (14,000  $\times$  g, 15 min, 10°C), the upper organic phase was collected and dried under nitrogen. For *LC-MS* analysis, dried lipids were reconstituted in 200  $\mu$ L isopropanol, vortexed, centrifuged (14,000  $\times$  g, 15 min, 10°C), and the supernatant collected. A pooled quality control (QC) sample was generated by combining equal aliquots from each lipid extract.

### LC-MS/MS analysis for lipids

Lipidomic analysis was performed according to the methods<sup>[21,22]</sup>. Briefly, samples were maintained at 10°C in an autosampler, with 3  $\mu$ L aliquots injected onto a reverse-phase CSH C18 column (Waters ACQUITY UPLC CSH C18; 1.7  $\mu$ m, 2.1  $\times$  100 mm) via a UPLC system (SHIMADZU, Japan). The mobile phase comprised Solvent A (acetonitrile–water, 6:4 v/v, 0.1% formic acid, 0.1 mM ammonium formate) and Solvent B (acetonitrile–isopropanol, 1:9 v/v, 0.1% formic acid, 0.1 mM ammonium formate), with a gradient starting at 30% Solvent B (300  $\mu$ L/min), held for 2 min, linearly increased to 100% Solvent B over 23 min, and equilibrated at 5% Solvent B for 10 min. Sample order was randomized to mitigate instrumentation bias. Post-separation, mass spectrometry was conducted on a Q-Exactive Plus (Thermo Scientific, USA) with shared parameters (heater 300°C, sheath gas 45 arb, auxiliary gas 15 arb, sweep gas 1 arb, capillary 350°C); For positive (ESI+) used 3.0 kV spray voltage, S-Lens RF 50%, and MS1 scan 200–1800 m/z, while for positive (ESI-) used 2.5 kV, S-Lens RF 60%, and MS2 scan 250–1800 m/z. Quality control samples were analyzed at each batch start and after every 5 samples to ensure data stability.

Raw data were processed using LipidSearch™ Software (v4.1, Thermo Fisher Scientific, CA, USA) for peak alignment, retention time correction, and peak area quantification. Analytical method validation was performed with key parameters set as follows: precursor tolerance = 5 ppm, product tolerance = 5 ppm, and product ion threshold = 5%. Lipid species exhibiting >30% relative standard deviation (RSD) or >50% missing values were excluded from the LipidSearch-extracted dataset. Following normalization and integration via Pareto scaling, processed data were subjected to principal component analysis (PCA) using SIMCA-P® software (v14.1, Umetrics, Umea, Sweden). Identified metabolites were annotated against the KEGG pathway database (<https://www.kegg.jp>).

genome.jp/kegg/pathway.html). Volcano plots were subsequently generated using R software.

## siRNA knockdown

Non-specific control siRNA and siRNAs for *FBXW7a* were purchased from GenePharma (Shanghai, China). Transfection of cells with the siRNA oligonucleotides was performed using Lipofectamine 2000 (Invitrogen, CA, USA) according to the manufacturer's instructions. The siRNAs used are listed here:

si NC: 5'-UUCUCCGAACGUGUCACGU-3'

si *FBXW7a*-1: 5'-GCTCCCTAAAGAGTTGGCACTCTAT-3'

si *FBXW7a*-2: 5'-ACAGGACAGUGUUUACAAATT-3'

## Western blot analysis

The western blotting protocol used has been described by us previously<sup>[23]</sup>. It can be briefly summarized as follows: the cells were washed with PBS, lysed with radio immune precipitation assay buffer for 30 min, and centrifuged at 12,000 rpm for 15 min (4oC). The supernatant was subjected to sodium dodecyl sulfate-polyacrylamide gel electrophoresis (SDS-PAGE) for separation of proteins, and the proteins were transferred to nitrocellulose (NC) membranes (0.45 µm, GE). The NC membranes were then blocked with non-fat milk and incubated with primary antibodies overnight at 4°C. Next, the membranes were washed with PBS and incubated with secondary antibodies (containing horseradish peroxidase) for 1–2 h. Following this, the membranes were washed with PBST, and the target proteins were detected with an imaging system from Bio-Rad (Hercules, CA, USA). Protein abundance was quantified using the ImageJ software.

## Quantitative qRT-PCR analysis

Total RNA was isolated using TRIzol reagent and reverse transcribed with the PrimerScript RT reagent kit. *qRT-PCR* analysis was performed with the TB Green *qRT-PCR* kit. The comparative Ct method was used to determine the relative quantity of the mRNA of the target gene, with the *GAPDH* gene as the internal control. The sequences of the primer pairs used are shown in Table 1.

Table 1 Primer sequences for *qRT-PCR*

Gene	Forward primer sequence (5'→3')	Reverse primer sequence (5'→3')
<i>HMOX1</i>	TGCTCAACATCCAGCTTTGA	AACTGTCGCCACCAGAAAGC
<i>SOD1</i>	ACAAAGATGGTGGCCGAT	AACGACTTCCAGCGTTTCCT
<i>NQO1</i>	GAAGAGCACTGATCGTACTGGC	GGATACTGAAAGTCGCAGGG
<i>Rictor</i>	CGAGTACGAGGGCGGAAT	ATCTGCCACATTTGGAGA
<i>GAPDH</i>	CAACGAATTGGCTACAGCA	AGGGGTCTACATGGCAACTG

## Detection of lipid ROS

Cells were seeded in 6-well plates or 24-well plates and were treated with trans-gnetin H for 24 h. The cells were then incubated with DCF-DA or 5 µM *BODIPY C11* at 37°C for 30 min. The cells in the 6-well plates were washed, and fluorescence intensity was detected by flow cytometry (BD FACSAria III, USA).

## Cell viability assay

For the determination of cell viability, cells were seeded in 96-well plates at a density of 104 cells/well and incubated with complete RPMI 1640 medium containing reagents. The medium was replaced with 100 µL fresh medium containing 10% CCK8 reagent, and this was followed by incubation for 3 h at 37°C. The plate was then read with a Synergy HT microplate reader (Bio-Tek, USA) (absorbance, 450 nm).

## Colony formation assay

Cells were seeded in 6-well plates at a density of 1000–2000 cells/well and treated with different combinations of regents. This was followed by culture in RPMI-1640 medium containing 10% FBS for 7 days. The colonies were then fixed with 4% paraformaldehyde, washed with PBS, and stained with crystal violet. All the assays were performed in triplicate.

## Autophagy analysis

Autophagy was detected using a previously described procedure<sup>[24]</sup>. Briefly, GFP-LC3 plasmids were transfected into cells, which were then treated with trans-gnetin H. The cells were fixed with 4% paraformaldehyde for 30 min and 0.1 M NH4Cl for 10 min and subsequently treated with 0.1% TritonX-100 and incubated with bovine serum albumin. Next, DAPI staining was performed, and the number of GFP-LC3 puncta was counted with a laser confocal microscope.

## Dead cell staining assay

The cytotoxicity of trans-gnetin H was determined using the dead cell staining assay test kit by treating cells with predetermined concentrations of trans-gnetin H for 24 h. Following this, the supernatant was discarded, and the cells were incubated with a working solution of propidium iodide (PI, 8 µM) for 30 min in the dark. The stained cells were then observed and imaged with a fluorescence microscope (OLYMPUS CKX53, Japan).

## Ferroptosis analysis

Cells were grown in 96-well plates until they reached 50%–60% confluence and exposed to different concentrations of RSL3 or erastin (for induction of ferroptosis), in combination with the indicated concentrations of trans-gnetin H. The effect of trans-gnetin H on ferroptosis was determined by assessing cell viability with the CCK8 kit in combination with the Synergy HT microplate reader (Bio-Tek, USA).

## Transmission electron microscopy

H1299 cell pellets were fixed in 2.5% electron microscopy-grade glutaraldehyde in 0.1M sodium cacodylate buffer (pH 7.4) at 4°C overnight. Cell sections were prepared by dehydration, embedding, and curing of the specimens, followed by 50-nm ultrathin section preparation and staining with uranyl acetate and lead citrate. These procedures followed previously described protocols<sup>[25]</sup>. The ultrathin specimens were examined, and images were acquired with a transmission electron microscope (HT7800, Japan).

## 2.16 Statistical analysis

The data distribution was assessed using the Shapiro-Wilk test in GraphPad Prism 9.0 for all datasets intended for parametric testing. Homogeneity of variances across groups was tested using Levene's test for all datasets intended for analysis via one-

way or two-way analysis of variance (ANOVA). Data were shown as mean  $\pm$  SEM. Statistical tests included unpaired one-tailed or two-tailed Student's t-test and one-way or two-way analysis of variance. *p* value 0.05 was considered statistically significant. In the graphed data \*, \*\* and \*\*\* denote *p* values of  $< 0.05$ , 0.01 and 0.001, respectively, ns, not significant.

## Results

### Trans-gnetin H promotes intracellular ROS generation

We first confirmed its growth-inhibitory effects in these models. Treatment dose-dependently reduced proliferation (Figure 1A, B), with peak efficacy at 10  $\mu$ M. To dissect the anti-proliferative mechanism, we performed untargeted lipidomics in HT29 cells (10  $\mu$ M, 2h). PCoA revealed profound metabolic reprogramming (Figure 1C), while volcano plots identified 395 dysregulated metabolites (171 upregulated; 406 downregulated; Figure 1D). KEGG enrichment highlighted glutathione metabolism upregulation (Figure 1E), suggesting oxidative stress.

**Figure 1**

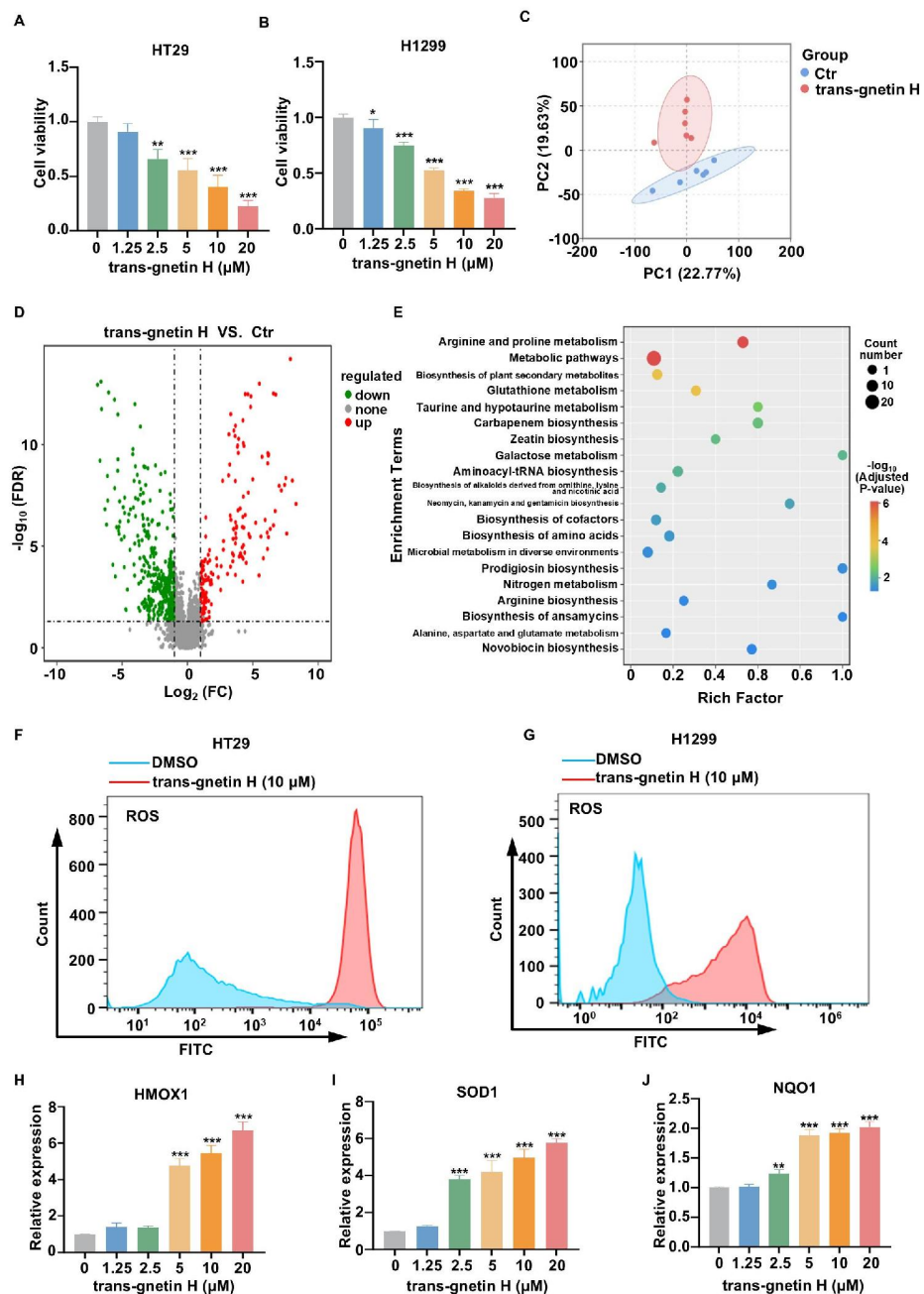


**Figure 1. Trans-gnetin H promotes intracellular ROS generation.** (A, B) HT29 (A) and H1299 (B) cells were treated with different concentrations of trans-gnetin H for 72 h, the viability of cells was detected by CCK8,  $n = 3$ , the number of technical or biological replicates performed. (C-E) Following 2 h treatment with 10  $\mu$ M trans-gnetin H, HT29 cells from treated and control groups ( $n=6$  per group, equal cell numbers) were collected. Lipids were extracted from each group and analyzed using untargeted liquid chromatography-mass spectrometry (LC-MS) for lipid species identification. (C) Principal component analysis (PCA) score plots distinguish the trans-gnetin H and control groups. (D) The volcano plot reveals 171 significantly upregulated and 406 significantly downregulated metabolites. (E) KEGG pathway analysis was performed on these differential metabolites. (F, G) HT29 (F) and H1299 (G) cells were treated with trans-gnetin H (10  $\mu$ M) for 2 h, and the ROS levels

were detected by FACS. (H-J) HT29 cells were treated with different concentrations of trans-gnetin H for 2 h, and the expression of *HMOX1* (H), *SOD1* (I), and *NQO1* (J) were detected by *qRT-PCR*. Data were analyzed by one-way ANOVA (A, B, H-J). \*p<0.05, \*\*p<0.01, \*\*\*p<0.001.

Notably, despite structural similarity to the ROS antagonist resveratrol, trans-gnetin H exhibited opposing redox activity, prompting our hypothesis of ROS-dependent growth inhibition. Validation studies showed trans-gnetin H significantly increased intracellular ROS in both H1299 and HT29 cells (Figure 1F, G). This pro-oxidant effect extended to breast (Figure S1A) and hepatocellular carcinoma (Figure S1B) models, suggesting potential broad-spectrum ROS induction across the colon, lung, breast, and hepatocellular carcinoma. Critically, trans-gnetin H concentration-dependently upregulated antioxidant genes (*HMOX1*, *SOD1*, *NQO1*), confirming ROS-mediated stress adaptation.

## Trans-gnetin H upregulates ROS-associated proteins to suppress mTOR activation

Building upon initial findings, we assessed trans-gnetin H's impact on ROS-regulatory proteins. Treatment concentration-dependently upregulated both the redox sensor *Nrf2* and its effector enzymes *HMOX1/SOD1/NQO1* at the protein level (Figure 2A & Figure S2A-D), aligning with prior transcriptional data.

To establish ROS-dependence of *Nrf2* induction, we employed ROS scavenger N-acetylcysteine (NAC). NAC co-treatment abolished *Nrf2* upregulation (Figure 2B & Figure S2B) and attenuated trans-gnetin H-induced expression of *HMOX1/SOD1/NQO1* mRNA (Figure 2C-E), with parallel effects on corresponding proteins (Figure 2B& Figure S2E-H). Thus, trans-gnetin H amplifies oxidative stress through coordinated *Nrf2* pathway activation.

Given established *mTORC1* modulation, we examined *mTORC2* components. Trans-gnetin H dose-dependently reduced *Rictor* (*mTORC2* core subunit) expression (Figure 2F,G) while suppressing mTORC2-mediated *AKT* Ser473 phosphorylation [26] and mTORC1-dependent *S6K* phosphorylation (Figure 2F,H & Figure S2I-L). Critically, NAC reversed all mTOR-related effects (Figure 2H & Figure S2K, L). Functionally, the *mTORC1* activator *MHY1485* rescued viability suppression in colony assays (Figure 2I, J). These data establish ROS-mediated dysregulation of both *mTOR* complexes by trans-gnetin H.

Figure 2

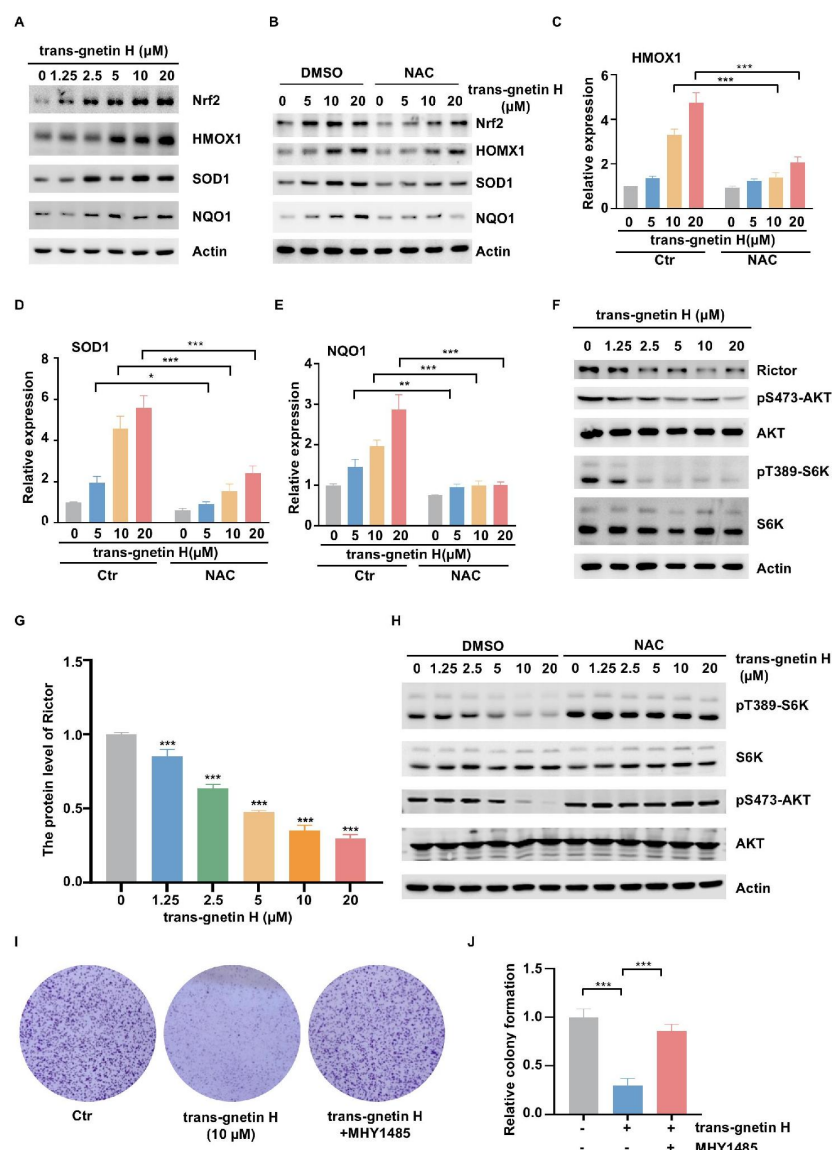


Figure 2. Trans-gnetin H upregulates ROS-associated proteins to suppress mTOR activation. (A) H1299 cells were treated with different concentrations of trans-gnetin H for 2 h, and the expression of *HMOX1* (H), *SOD1* (I), and *NQO1* (J) were detected by *qRT-PCR*. Data were analyzed by one-way ANOVA (A, B, H-J). \*p<0.05, \*\*p<0.01, \*\*\*p<0.001.

trans-gnetin H for 2 h, and the indicated proteins were evaluated by western blot. (B) H1299 cells were treated with different concentrations of trans-gnetin H or NAC (2 mM) for 2 h, and the indicated proteins were evaluated by western blot. (C-E) H1299 cells were treated with different concentrations of trans-gnetin H or NAC (2 mM) for 2 h, and then the expression of *HMOX1* (C), *SOD1* (D), and *NQO1* (E) were detected by qRT-PCR. (F, G) HT29 cells were treated with different concentrations of trans-gnetin H for 2 h, and the indicated proteins were evaluated by western blot (F), quantitative for Rictor (G) is presented. (H) H1299 cells were treated with different concentrations of trans-gnetin H or NAC (2 mM) for 2 h, and the indicated proteins were evaluated by western blot. (I, J) HT29 cells were treated with trans-gnetin H (10  $\mu$ M) or *MHY1485* (10 nM), and the cell death was detected by colony formation assay (I), quantitative data are presented in (J). Data were analyzed by one-way ANOVA (G), two-way ANOVA (C-E, J). \*p < 0.05, \*\*p < 0.01, \*\*\*p < 0.001.

## Trans-gnetin H promotes the degradation of Rictor via ROS

We next investigated the mechanism through which trans-gnetin H mediates the decrease in *Rictor*. However, we found that trans-gnetin H does not regulate *Rictor* expression at the transcriptional level (Figure 3A). To determine whether trans-gnetin H regulates *Rictor* at the post-translational level, we treated cells with CHX, an inhibitor of mRNA translation, and found that trans-gnetin H significantly shortens the half-life of *Rictor* (Figure 3B,C). Numerous previous studies have shown that the half-life of proteins is mainly regulated by ubiquitination<sup>[27-29]</sup>. Accordingly, our results showed that trans-gnetin H could significantly promote the ubiquitination of *Rictor*. Moreover, we found that the promotive effect of trans-gnetin H on *Rictor* degradation could be blocked by NAC treatment (Figure 3D,E), and the addition of NAC inhibited trans-gnetin-mediated ubiquitination of *Rictor* (Figure 3F).

It has been shown that ubiquitination of *Rictor* is mainly regulated by *FBXW7 $\alpha$* <sup>[30]</sup>. Therefore, we transfected cells with two siRNAs that specifically target *FBXW7 $\alpha$*  and found that knockdown of *FBXW7 $\alpha$*  blocked trans-gnetin H-mediated *Rictor* degradation (Figure 3G,H). These results indicate that trans-gnetin H facilitates *FBXW7 $\alpha$* -mediated ubiquitination of *Rictor* via ROS, which in turn, promotes *Rictor* degradation.

**Figure 3**

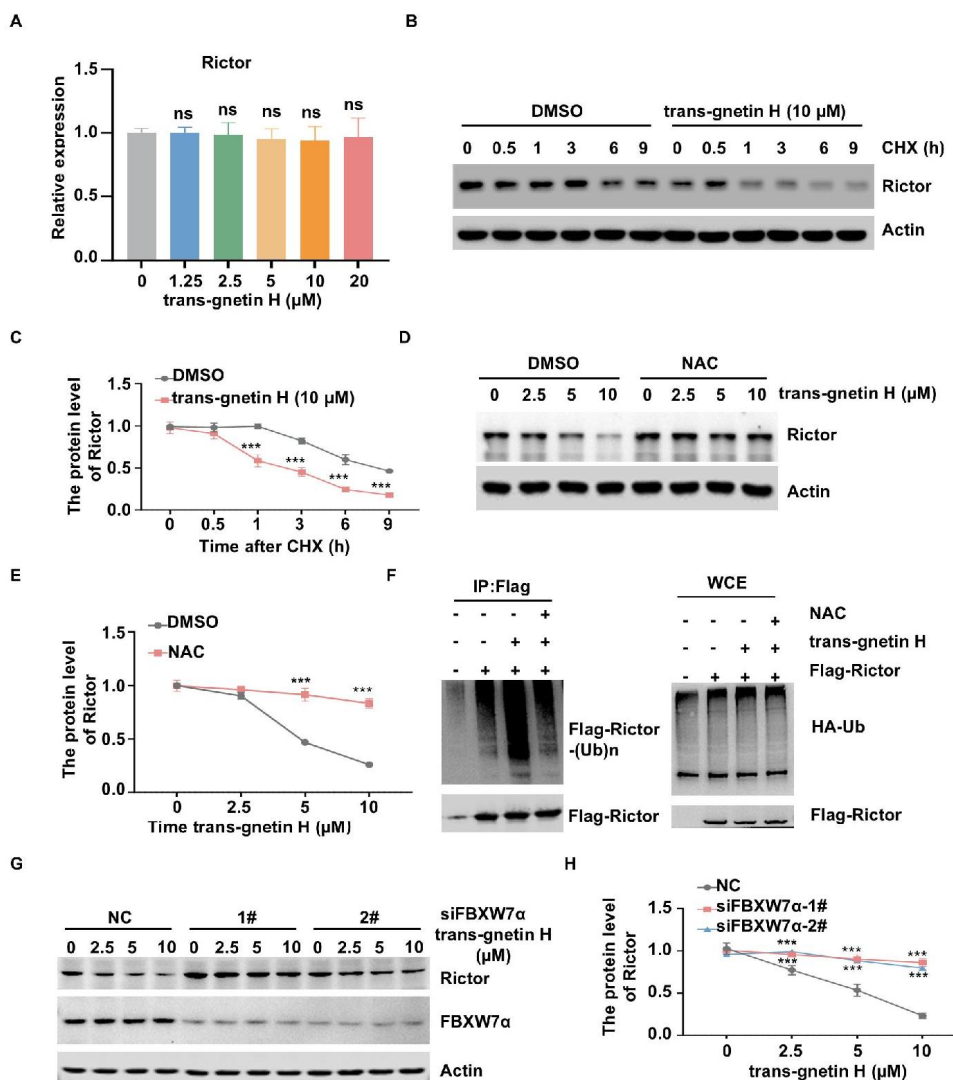


**Figure 3. Trans-gnetin H promotes the degradation of Rictor via ROS.** (A) HT29 cells were treated with different concentrations of trans-gnetin H for 2 h, and the mRNA of *Rictor* were evaluated by qRT-PCR. (B, C) HT29 cells were treated with trans-gnetin H (10  $\mu$ M) or CHX (25 mg/ $\mu$ L) for indicated time, and the indicated proteins were evaluated by western blot (B), quantitative data for *Rictor* are presented in (C). (D, E) HT29 cells were treated with different concentrations of trans-gnetin H or NAC (2 mM) for 2 h, and the indicated proteins were evaluated by western blot (D), quantitative data for *Rictor* are presented in (E). (F) HT29 cells

were treated with trans-gnetin H (10  $\mu$ M) or NAC (2 mM) for 2 h, and the *Rictor* ubiquitination was analyzed by western blot. (G, H) FBXW7 $\alpha$ -knockdown HT29 cells were treated with different concentrations of trans-gnetin H for 2 h, and the indicated proteins were evaluated by western blot (G), quantitative data for *Rictor* are presented in (H). Data were analyzed by one-way ANOVA (A), two-way ANOVA (C, E, H). n = 3, the number of independent experiments performed. \*p < 0.05, \*\*p < 0.01, \*\*\*p < 0.001.

## Trans-gnetin H does not affect cell ferroptosis

To determine whether trans-gnetin H can regulate cell ferroptosis, we investigated the regulatory effects of trans-gnetin H on lipid ROS production and mitochondrial morphology. Our results demonstrated that trans-gnetin H had no influence on intracellular lipid ROS generation (Figure 4A,B), even though it significantly promoted ROS generation. Further, trans-gnetin H did not affect mitochondrial morphological characteristics either (Figure 4C). In accordance with these results, trans-gnetin H did not play a role in sensitivity to erastin (a known inducer of cell ferroptosis) and RSL3-induced ferroptosis (Figure 4D, E). These results suggest that trans-gnetin H is not involved in cell ferroptosis.

**Figure 4**

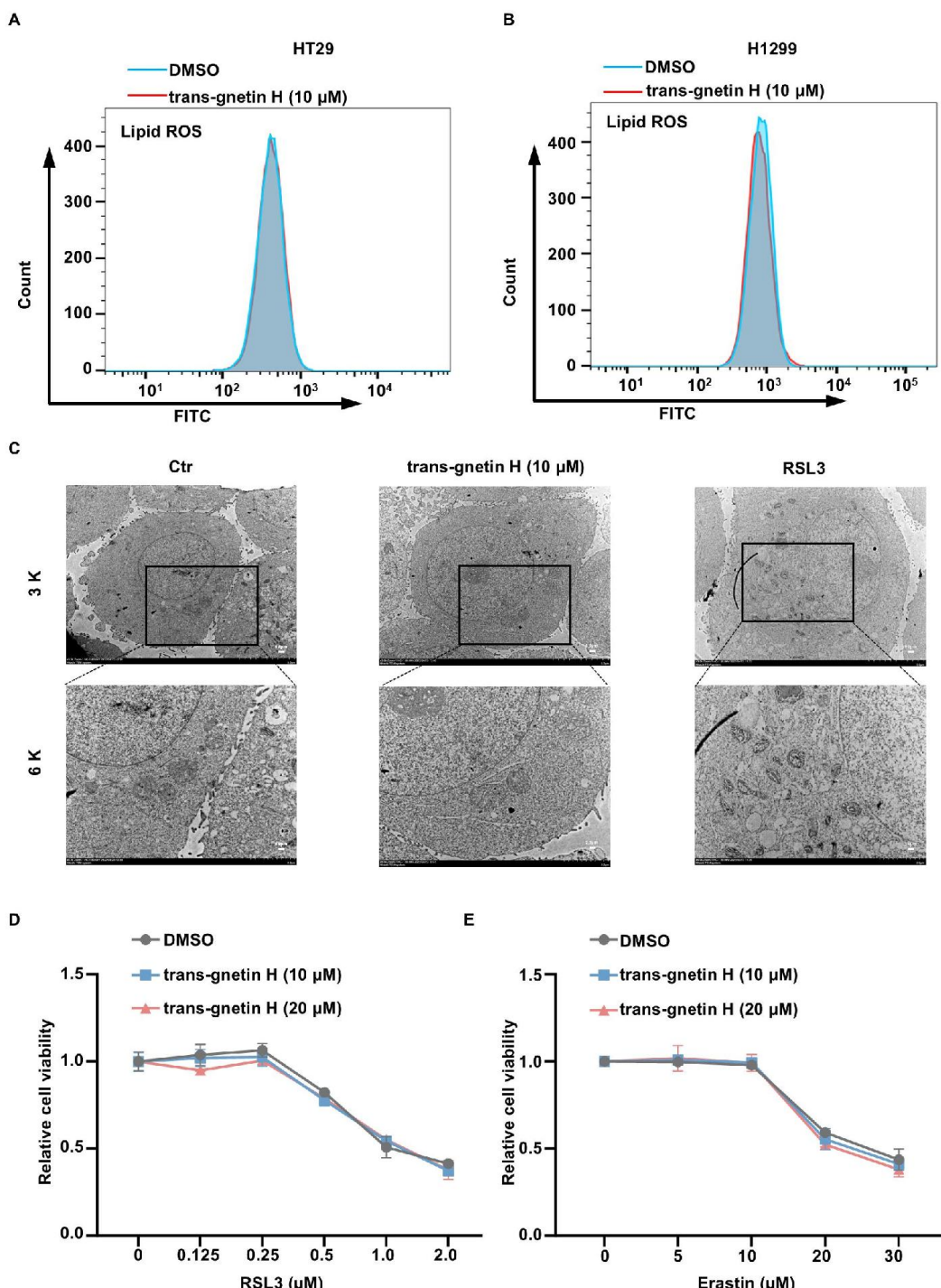


**Figure 4. Trans-gnetin H does not affect cell ferroptosis.** (A, B) HT29 (A) and H1299 (B) cells were treated with the trans-gnetin H (10  $\mu$ M) for 2 h, and the lipid ROS was analyzed by FACS. (C) H1299 cells were treated with the trans-gnetin H (10  $\mu$ M) or RSL3 ( $\mu$ M) for 12 h, and analyze the ultrastructure of mitochondria with transmission electron microscopy. (D, E) H1299 cells were treated with different concentrations of trans-gnetin H, RSL3 (D) for 24 h or erastin (E) for 24 h, and the

viability of indicated cells was examined using CCK8.

## Trans-gnetin H regulates cell viability via ROS

The results of our PI staining experiments on H1299 cells demonstrated that trans-gnetin H significantly inhibited cell growth, and this effect could be blocked by NAC (Figure 5A). Consistent results were obtained with the CCK8 assay (Figure 5B). Moreover, we found that knockdown of *FBXW7α* blocked the inhibitory effect of trans-gnetin H on cell viability (Figure 5C). In our previous study, we found that trans-gnetin H could regulate cellular autophagy<sup>[5]</sup>. Consistent with the previous findings, trans-gnetin H demonstrated the ability to significantly promote autophagy (Figure 5D,E). Further, the addition of NAC could block trans-gnetin H-induced autophagy (Figure 5D,E), and knockdown of *FBXW7α* inhibited the induction of autophagy by trans-gnetin H (Figure 5F,G). Thus, these results suggest that trans-gnetin H has the ability to inhibit cell viability and induce autophagy through pathways that involve ROS and *FBXW7α* (which mediates ubiquitination of *Rictor*).

**Figure 5**

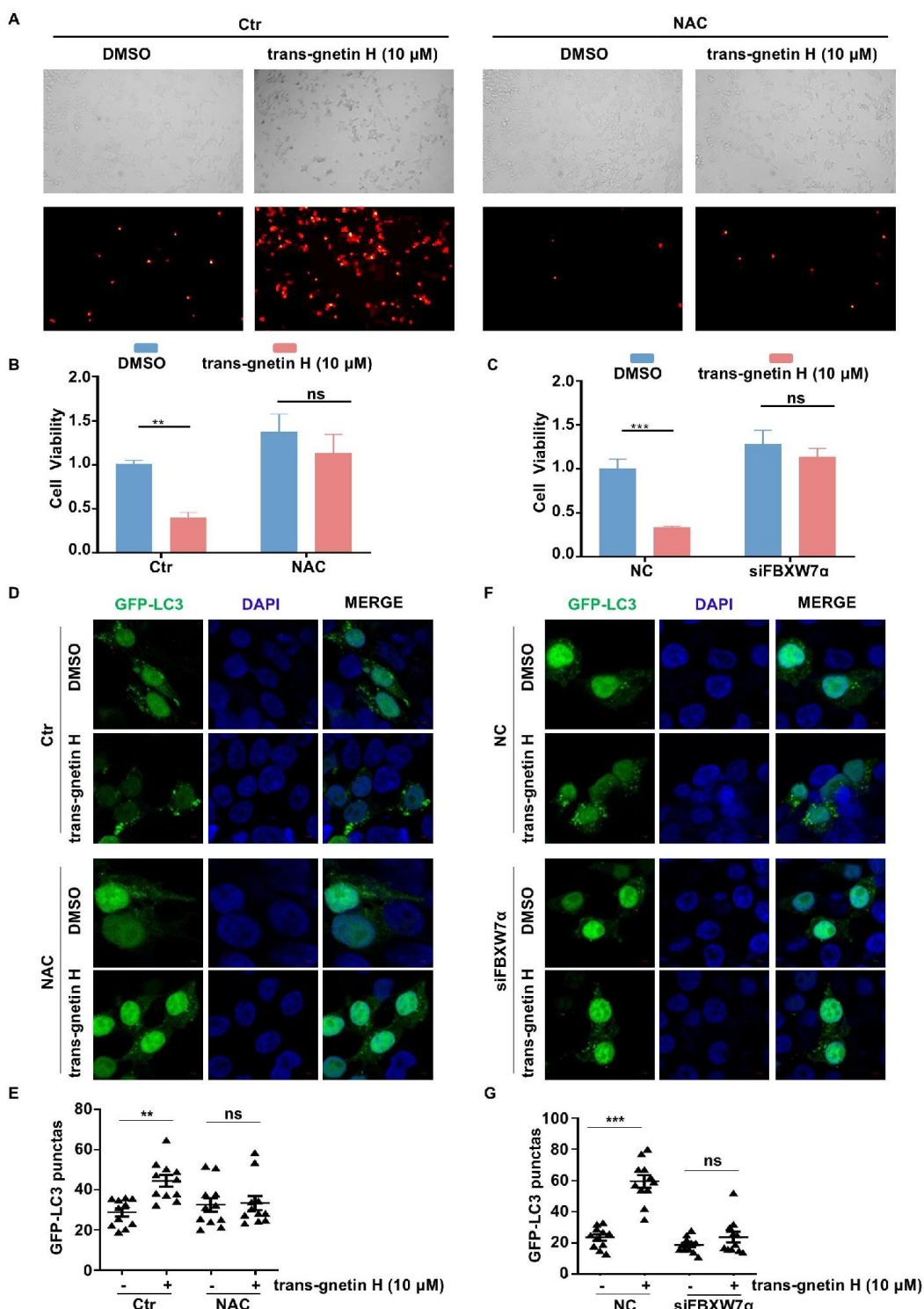


**Figure 5. Trans-gnetin H regulates cell viability via ROS.** (A) H1299 cells were treated with the trans-gnetin H (10  $\mu$ M) for 2 h, and the dead cell was detected by staining assay. (B) HT29 cells were treated with the trans-gnetin H (10  $\mu$ M) or NAC for 2 h, and the cell viability was detected by CCK8. (C) FBXW7 $\alpha$ -knockdown HT29 cells were treated with trans-gnetin H for 2 h, and the cell viability was detected by CCK8. (D, E) HT29 cells were treated with the trans-gnetin H (10  $\mu$ M) or

NAC (2 mM) for 2 h, and autophagy was detected by GFP-LC3 puncta (D), quantitative data for GFP-LC3 puncta are presented in (E). (F, G) FBXW7 $\alpha$ -knockdown HT29 cells were treated with trans-gnetin H (10  $\mu$ M) for 2 h, and autophagy was detected by GFP-LC3 puncta (F), quantitative data for GFP-LC3 puncta are presented in (G). n = 3, the number of technical or biological replicates performed. \*p < 0.05, \*\*p < 0.01, \*\*\*p < 0.001.

## 4. Discussion

In the present study, we provide confirmatory evidence for the effect of trans-gnetin H on the cell viability of cancer cells. Further, we demonstrate that the underlying mechanisms involve the inhibition of mTORC1 and mTORC2 activity via the ROS-Rictor signaling axis. Specifically, our results show that trans-gnetin H-induced ROS can regulate mTORC1 activity through the FBXW7 $\alpha$ -Rictor-mTORC2-AKT signaling axis: that is, ROS can enhance FBXW7 $\alpha$ -mediated ubiquitination and degradation of Rictor, which in turn inhibits mTORC2 and mTORC1 activity. This is a novel mechanism of trans-gnetin H that has not been reported so far, so the findings have significant implications in terms of the future therapeutic potential of trans-gnetin H.

As trans-gnetin H is a trimer of resveratrol, it seems logical that it would have stronger scavenging ability than resveratrol. In contrast, we found that trans-gnetin H promotes the production of cellular ROS and enhances the expression of the *Nrf2* protein, which is an important effector protein that plays a role in the response to ROS and is an important indicator of intracellular ROS changes<sup>[31]</sup>. In addition, we also found the trans-gnetin H upregulates the expression of the downstream *Nrf2* antioxidant proteins *HMOX1*, *SOD1*, and *NQO1*. Further, when the cells were pre-treated with NAC before exposure to trans-gnetin H, this effect was inhibited. This suggests that contrary to the previously reported ROS clearance function of resveratrol, trans-gnetin H significantly promotes intracellular ROS production while enhancing intracellular antioxidant protein expression. Thus, although trans-gnetin H is composed of resveratrol, it does not possess all the characteristics of resveratrol.

Resveratrol trimers exhibit a broad spectrum of bioactivities attributed to their structural diversity. Miyabenol C demonstrates notable multi-target pharmacological activities: inducing anti-proliferative and apoptotic effects in tumor cells; inhibiting protein kinase C (PKC); antagonizing the human serotonin (5-HT) receptor; mediating estrogen-like effects via estrogen receptor binding; and exhibiting antagonistic activity toward ecdysone in *Drosophila* cell models. Significantly, Miyabenol C has been identified as a potent inhibitor of  $\beta$ -secretase (BACE1). It effectively suppresses the pathological production of  $\beta$ -amyloid (A $\beta$ ) in both in vitro and in vivo model systems, strongly suggesting its therapeutic potential for central nervous system neurodegenerative disorders such as Alzheimer's disease<sup>[32]</sup>. Further research revealed that the antitumor effects of another trimer, pauciflorol B, are primarily mediated through activation of the p53 signaling pathway, thereby regulating cellular apoptosis and senescence<sup>[33]</sup>. In contrast, the trimer  $\alpha$ -viniferin displays selective antibacterial activity, exhibiting potent inhibition against *Staphylococcus aureus* and *Escherichia coli*, while demonstrating comparatively weaker activity against *Salmonella Paratyphi*<sup>[34]</sup>. These examples highlight the functional heterogeneity among resveratrol oligomers and underscore the unique ROS-promoting and mTOR-inhibitory properties of trans-gnetin H identified in our study.

In our next set of experiments, we tried to elucidate the potential mechanism underlying intracellular ROS production induced by trans-gnetin H. First, we tried to detect changes in the function of the four complexes in the mitochondrial respiratory chain, but we found that trans-gnetin H did not affect this mechanism of ROS production. Studies have shown that lipid overload-induced toxicity and insulin resistance is one of the mechanisms that drives ROS production, and cholesterol and oxidized sterols can also cause mitochondrial dysfunction and ROS production<sup>[35]</sup>. However, our non-targeted lipidomics analysis of trans-gnetin H-treated cells showed that there was no increase in cholesterol and fatty acids after trans-gnetin H treatment. Thus, the mitochondrial and lipid overload mechanisms of intracellular ROS production were ruled out as the ROS induction pathways of trans-gnetin H.

We next analyzed the molecular structure of trans-gnetin H and found a large number of hydroxyl groups (-OH). Based on this observation, we speculated that hydroxyl radicals released from trans-gnetin H may account for the increase in ROS observed in cells treated with trans-gnetin H. In addition, we analyzed the phenotype at the cellular level, and our results showed that the expression of superoxide dismutase and catalase was significantly inhibited by trans-gnetin H. Superoxide dismutase binds to the superoxide by-products of oxidative phosphorylation and converts them to hydrogen peroxide and diatomic oxygen. Thus, changes in these enzymes may also be an important factor in the promotion of ROS production by trans-gnetin H.

In our previous studies, trans-gnetin H was found to inhibit mTORC1 activity by activating the AMPK pathway<sup>[5]</sup>. In this study, we also wanted to explore whether trans-gnetin H has an effect on mTORC2. Our results show that trans-gnetin H significantly suppressed the phosphorylation of *AKT* at *Ser473*, which is a conserved site for mTORC2-mediated phosphorylation on *AKT*<sup>[26]</sup>. Thus, our results suggest that trans-gnetin H can also significantly inhibit mTORC2 activity. We wanted to learn more about how trans-gnetin H performs this function. Our previous study showed that vitamin C-induced ROS regulated mTORC2 activation by promoting the degradation of *Rictor*<sup>[36]</sup>, which is an important component protein of mTORC2<sup>[37]</sup>. Building upon these findings, we further investigated the effect of trans-gnetin H on *Rictor*. Our data demonstrate that trans-gnetin H inhibits mTORC2 activity by inducing intracellular ROS generation, which activates the ubiquitin ligase FBXW7 $\alpha$ . This activation triggers ubiquitination and subsequent proteasomal degradation of the mTORC2 component *Rictor*. Notably, although trans-gnetin H potently induced FBXW7 $\alpha$ -mediated *Rictor* ubiquitination and degradation, it failed to enhance the FBXW7 $\alpha$ -Rictor physical interaction in co-immunoprecipitation assays (Figure S3A). This finding suggests that trans-gnetin H/ROS facilitates *Rictor* ubiquitination through mechanisms independent of strengthening the FBXW7 $\alpha$ -Rictor binding affinity. While this dissociation between binding affinity and degradation efficiency warrants further investigation, it is well-established that mTORC2 regulates mTORC1 activ-

ity via *AKT* phosphorylation at *Ser473*. This established link aligns with our prior observation of trans-gnetin H-mediated *mTORC1* inhibition. Therefore, collectively, our findings indicate that trans-gnetin H suppresses *mTORC1* activity through dual pathways: *AMPK* activation and *mTORC2* inhibition.

Further supporting this proposed mechanism, our supplementary experiments revealed that trans-gnetin H significantly upregulates *FBXW7* protein expression (Figure S3B). This finding indicates that trans-gnetin H not only facilitates *FBXW7*-mediated ubiquitination and degradation of *Rictor* but may also potentiate *FBXW7*'s regulatory effect on *Rictor* by directly enhancing *FBXW7* expression. Within cellular systems, *FBXW7* exists as three distinct isoforms: the  $\alpha$  isoform localizes predominantly to the nucleus, the  $\beta$  isoform exhibits cytoplasmic distribution, and the  $\gamma$  isoform primarily resides within the nucleolus<sup>[38]</sup>. Given this broad subcellular distribution of *FBXW7*, examining only its subcellular localization may be insufficient to elucidate the precise mechanism by which trans-gnetin H or ROS regulate *FBXW7*-mediated *Rictor* degradation. It is extensively documented that *GSK3 $\beta$* -mediated phosphorylation of *Rictor* triggers *FBXW7*-dependent degradation<sup>[30]</sup>. Although this study did not directly assess *FBXW7* phosphorylation status, our functional analyses demonstrate that trans-gnetin H-induced ROS promotes *Rictor* degradation specifically through *FBXW7 $\alpha$* —highlighting a central finding of this work. Therefore, post-translational modifications (PTMs) of *FBXW7 $\alpha$* , such as phosphorylation, represent a plausible regulatory mechanism through which ROS may modulate its activity, constituting a significant direction for future investigations.

Autophagy is a highly conserved self-degrading system induced primarily by nutritional deprivation or stress<sup>[35]</sup>. It contributes to the maintenance of cellular homeostasis by promoting the degradation of intracellular protein aggregates, organelles, and other macromolecules<sup>[39]</sup>. Abnormalities in autophagy may induce the initiation phase of tumorigenesis. In the later stages of tumor development, autophagy is essential for obtaining nutrients and dealing with the unfavorable tumor microenvironment<sup>[40]</sup>. Our previous study showed that trans-gnetin H can promote autophagy via inhibition of the *mTORC1-TFEB* signaling axis to facilitate the localization of *TFEB* within the nucleus<sup>[5]</sup>. *TFEB* belongs to a class of transcription factors that have been reported to regulate lysosomal biogenesis and autophagic gene expression<sup>[41]</sup>. In the present study, we have expanded on the related mechanisms by reporting that trans-gnetin H-promoted autophagy is highly dependent on ROS. Further, we found that the promotive effect of ROS on autophagy was brought about via suppression of the *mTOR* pathway. By combining our present findings with our previous findings, we can deduce that trans-gnetin H promotes autophagy through the *mTOR/AMPK/ROS* axis. In the future, it would be interesting to explore the mechanisms involved as a way of identifying potential treatment targets.

Elevated ROS is an important feature of cell ferroptosis, and lipid ROS and mitochondrial crinkling represent the gold standard for detecting cell ferroptosis<sup>[42]</sup>. In this study, we tried to find evidence that trans-gnetin H regulates ferroptosis in cells. As shown in Figure 4, although trans-gnetin H did result in a significant increase in the generation of intracellular ROS and had a broad spectrum of

other effects, it did not induce the production of intracellular lipid ROS (elevated lipid ROS is an important condition for ferroptosis). In addition, our experimental results show that trans-gnetin H has no obvious destructive effect on the mitochondria in the cell. Importantly, our ferroptosis assay showed that trans-gnetin H did not cause ferroptosis in cells. In line with the present findings, in our previous study, too, we ruled out the ability of trans-gnetin H to cause apoptosis. In summary, we believe that the production of intracellular ROS induced by trans-gnetin H inhibits the activity of *mTOR* and activates autophagy, similar to our previous study.

In this paragraph, we will highlight some of the questions that are still to be answered in the future and some limitations of our study. The selection of cancer cell lines in this study was strategically aligned with global cancer burden data. The four cell lines investigated—NCI-H1299 (lung cancer), HT29 (colorectal cancer), HepG2 (liver cancer), and MDA-MB-231 (breast cancer)—represent malignancies ranked highest in global incidence and mortality: lung cancer ranks first in mortality, colorectal cancer third in incidence, liver cancer second in mortality, and breast cancer first in incidence<sup>[43]</sup>. These cancers collectively span major physiological systems (respiratory, digestive, and reproductive), enhancing the translational relevance of our findings across diverse human cancers. However, it is important to note that while our initial screening included MDA-MB-231 and HepG2 cells, our subsequent detailed mechanistic investigations focused primarily on H1299 and HT29 models. Consequently, the generalizability of the specific ROS-Rictor-mTOR signaling axis identified in this study to breast cancer (MDA-MB-231) and liver cancer (HepG2) cells remains to be fully characterized and constitutes a limitation of this work. Additionally, the experiments were conducted at the cellular level and need to be verified through *in vivo* studies in the future, especially for evaluating the side effects of trans-gnetin H. Our cellular models inherently overlook tumor microenvironment complexity and interpatient heterogeneity within each cancer type. For instance, while MDA-MB-231 represents triple-negative breast cancer, other molecular subtypes (e.g., HER2+, ER+) may respond differently<sup>[44]</sup>. Similarly, the reliance on single cell lines per cancer type limits extrapolation to intratumoral genomic diversity. Future studies incorporating primary patient-derived cells, co-culture systems, and *in vivo* models will be essential to confirm pathophysiological relevance. At the level of mechanism analysis, our previous study showed that *mTORC1* can be inhibited by trans-gnetin H<sup>[5]</sup>, and in our present study, trans-gnetin H was found to have the ability to inhibit both *mTORC1* and *mTORC2* activity via ROS, as well as the viability of the cancer cell lines examined. While these findings indicate the potential anti-tumor effects of trans-gnetin H, it is not clear which upstream signaling molecule of *mTOR* is targeted by trans-gnetin H-induced ROS. Current studies on the upstream signaling molecules of *mTORC1* focus on amino acids, growth factors, and glucose<sup>[45]</sup>, so they might shed light on the potential targets of trans-gnetin H-induced ROS. In the future, this line of investigation might help identify therapeutic targets for cancer treatment. In our previous study, we also found that trans-gnetin H inhibited *mTORC1* activity through *AMPK*<sup>[5]</sup>, but in this study, we did not investigate the relationship between ROS and the *AMPK* pathway. Thus, it

is not clear whether ROS can regulate *mTOR* through the *AMPK* pathway, or whether the regulation of the ROS-FBXW7 $\alpha$ -Rictor axis is dependent on *AMPK* signaling. Another limitation was that although we found that ROS can promote FBXW7 $\alpha$ -mediated ubiquitination and degradation of *Rictor*, we did not clarify the mechanism of ROS regulation of *FBXW7 $\alpha$* . Thus, whether ROS promotes the expression of *FBXW7 $\alpha$*  or regulates its stability is a topic that warrants investigating. Another shortcoming of the present study is that we have not explored whether trans-gnetin H can cause pyroptosis and necrotic apoptosis, which is a topic we hope to explore in subsequent studies.

In summary, the present findings reveal that trans-gnetin H inhibits tumor cell viability through the following pathway: trans-gnetin H-induced increase in ROS production leads to FBXW7 $\alpha$ -mediated ubiquitination degradation of *Rictor*; this further leads to inhibition of *mTORC2* activity that, in turn, inhibits *mTORC1* activity via inhibition of *AKT* phosphorylation. With regard to the underlying mechanism, we were able to add to the literature by demonstrating that trans-gnetin H can regulate cell viability and autophagy through its effects on ROS and *FBXW7 $\alpha$* .

## Reference

1. C. Lennicke, H.M. Cocheme, Redox metabolism: ROS as specific molecular regulators of cell signaling and function, *Mol Cell* 81(18) (2021) 3691-3707.
2. B. Singla, R. Holmdahl, G. Csanyi, Editorial: Oxidants and Redox Signaling in Inflammation, *Front Immunol* 10 (2019) 545.
3. D.D. Roberts, Extracellular Matrix and Redox Signaling in Cellular Responses to Stress, *Antioxid Redox Signal* 27(12) (2017) 771-773.
4. C.K. Sen, S. Roy, Redox signals in wound healing, *Biochim Biophys Acta* 1780(11) (2008) 1348-61.
5. C. Xia, G. Wang, L. Chen, H. Geng, J. Yao, Z. Bai, L. Deng, Trans-gnetin H isolated from the seeds of *Paeonia* species induces autophagy via inhibiting mTORC1 signalling through AMPK activation, *Cell Prolif* (2022) e13360.
6. Y. Gao, C. He, R. Ran, D. Zhang, D. Li, P.G. Xiao, E. Altman, The resveratrol oligomers, cis- and trans-gnetin H, from *Paeonia suffruticosa* seeds inhibit the growth of several human cancer cell lines, *J Ethnopharmacol* 169 (2015) 24-33.
7. J. Zhang, K. Ma, T. Qi, X. Wei, Q. Zhang, G. Li, J.F. Chiu, P62 regulates resveratrol-mediated Fas/Cav-1 complex formation and transition from autophagy to apoptosis, *Oncotarget* 6(2) (2015) 789-801.
8. C.H. Chang, C.Y. Lee, C.C. Lu, F.J. Tsai, Y.M. Hsu, J.W. Tsao, Y.N. Juan, H.Y. Chiu, J.S. Yang, C.C. Wang, Resveratrol-induced autophagy and apoptosis in cisplatin-resistant human oral cancer CAR cells: A key role of AMPK and Akt/mTOR signaling, *Int J Oncol* 50(3) (2017) 873-882.
9. Y. Qin, Z. Ma, X. Dang, W. Li, Q. Ma, Effect of resveratrol on proliferation and apoptosis of human pancreatic cancer MIA PaCa-2 cells may involve inhibition of the Hedgehog signaling pathway, *Mol Med Rep* 10(5) (2014) 2563-7.
10. J.Y. Jang, E. Im, N.D. Kim, Mechanism of Resveratrol-Induced Programmed Cell Death and New Drug Discovery against Cancer: A Review, *Int J Mol Sci* 23(22) (2022).
11. J. Yang, X. Zhou, X. Zeng, O. Hu, L. Yi, M. Mi, Resveratrol attenuates oxidative injury in human umbilical vein endothelial cells through regulating mitochondrial fusion via TyrRS-PARP1 pathway, *Nutr Metab (Lond)* 16 (2019) 9.
12. C. Tan, H. Zhou, X. Wang, K. Mai, G. He, Resveratrol attenuates oxidative stress and inflammatory response in turbot fed with soybean meal based diet, *Fish Shellfish Immunol* 91 (2019) 130-135.
13. K. Szkudelska, M. Okulicz, I. Hertig, T. Szkudelski, Resveratrol ameliorates inflammatory and oxidative stress in type 2 diabetic Goto-Kakizaki rats, *Biomed Pharmacother* 125 (2020) 110026.
14. S.C. Chao, Y.J. Chen, K.H. Huang, K.L. Kuo, T.H. Yang, K.Y. Huang, C.C. Wang, C.H. Tang, R.S. Yang, S.H. Liu, Induction of sirtuin-1 signaling by resveratrol induces human chondrosarcoma cell apoptosis and exhibits antitumor activity, *Sci Rep* 7(1) (2017) 3180.
15. Z. Liu, X. Wu, J. Lv, H. Sun, F. Zhou, Resveratrol induces p53 in colorectal cancer through SET7/9, *Oncol Lett* 17(4) (2019) 3783-3789.
16. S.H. Lee, Y.J. Lee, Synergistic anticancer activity of resveratrol in combination with docetaxel in prostate carcinoma cells, *Nutr Res Pract* 15(1) (2021) 12-25.
17. S. Battaglioni, D. Benjamin, M. Wälchli, T. Maier, M.N. Hall, mTOR substrate phosphorylation in growth control, *Cell* 185(11) (2022) 1814-1836.
18. G. Wang, L. Chen, S. Qin, T. Zhang, J. Yao, Y. Yi, L. Deng, Mechanistic Target of Rapamycin Complex 1: From a Nutrient Sensor to a Key Regulator of Metabolism and Health, *Adv Nutr* 13(5) (2022) 1882-1900.
19. Y.K. He, X.T. Cen, S.S. Liu, H.D. Lu, C.N. He, Protective effects of ten oligostilbenes from *Paeonia suffruticosa* seeds on interleukin-1 $\beta$ -induced rabbit osteoarthritis chondrocytes, *BMC Chem* 13(1) (2019) 72.
20. V. Matyash, G. Liebisch, T.V. Kurzhalia, A. Shevchenko, D. Schwudke, Lipid extraction by methyl-tert-butyl ether for high-throughput lipidomics, *J Lipid Res* 49 (2008) 1137-1146.
21. M. Holcapek, G. Liebisch, K. Ekroos, Lipidomic analysis, *Anal Bioanal Chem* 90 (2020) 4249-4257.
22. C. Wang, Y. Tong, Y. Wen, J. Cai, H. Guo, L. Huang, Hepatocellular carcinoma-associated protein td26 interacts and enhances sterol regulatory element-binding protein 1 activity to promote tumor cell proliferation and growth, *Hepatology* 68 (2018) 1833-1850.
23. G. Wang, S. Qin, Y. Zheng, C. Xia, P. Zhang, L. Zhang, J. Yao, Y. Yi, L. Deng, T-2 Toxin Induces Ferroptosis by Increasing Lipid Reactive Oxygen Species (ROS) and Downregulating Solute Carrier Family 7 Member 11 (SLC7A11), *J Agric Food Chem* 69(51) (2021) 15716-15727.
24. L. Deng, C. Jiang, L. Chen, J. Jin, J. Wei, L. Zhao, M. Chen, W. Pan, Y. Xu, H. Chu, X. Wang, X. Ge, D. Li, L. Liao, M. Liu, L. Li, P. Wang, The ubiquitination of rag A GTPase by RNF152 negatively regulates mTORC1 activation, *Mol Cell* 58(5) (2015) 804-818.
25. H. Lee, F. Zandkarimi, Y. Zhang, J.K. Meena, J. Kim, L. Zhuang, S. Tyagi, L. Ma, T.F. Westbrook, G.R. Steinberg, D. Nakada, B.R. Stockwell, B. Gan, Energy-stress-mediated AMPK activation inhibits ferroptosis, *Nat Cell Biol* 22(2) (2020) 225-234.
26. D.D. Sarbassov, D.A. Guertin, S.M. Ali, D.M. Sabatini, Phosphorylation and regulation of Akt/PKB by the rictor-mTOR complex, *Science* 307(5712) (2005) 1098-101.
27. L. Deng, T. Meng, L. Chen, W. Wei, P. Wang, The role of ubiquitination in tumorigenesis and targeted drug discovery, *Signal Transduct Target Ther* 5(1) (2020) 11.

28. S. Bae, S.Y. Kim, J.H. Jung, Y. Yoon, H.J. Cha, H. Lee, K. Kim, J. Kim, I.S. An, J. Kim, H.D. Um, I.C. Park, S.J. Lee, S.Y. Nam, Y.W. Jin, J.H. Lee, S. An, Akt is negatively regulated by the MULAN E3 ligase, *Cell Res* 22(5) (2012) 873-85.
29. J.H. Mao, I.J. Kim, D. Wu, J. Climent, H.C. Kang, R. DelRosario, A. Balmain, FBXW7 targets mTOR for degradation and cooperates with PTEN in tumor suppression, *Science* 321(5895) (2008) 1499-502.
30. J. Koo, X. Wu, Z. Mao, F.R. Khuri, S.Y. Sun, Rictor Undergoes Glycogen Synthase Kinase 3 (GSK3)-dependent, FBXW7-mediated Ubiquitination and Proteasomal Degradation, *J Biol Chem* 290(22) (2015) 14120-9.
31. A.T. Dinkova-Kostova, I.M. Copple, Advances and challenges in therapeutic targeting of NRF2, *Trends Pharmacol Sci* (2023).
32. J. Hu, T. Lin, Y. Gao, J. Xu, C. Jiang, G. Wang, G. Bu, H. Xu, H. Chen, Y. Zhang, The resveratrol trimer miyabenol C inhibits  $\beta$ -secretase activity and  $\beta$ -amyloid generation, *PLoS One* 10(1) (2015) e0115973.
33. H. Qiao, X. Chen, L. Xu, J. Wang, G. Zhao, Y. Hou, H. Ge, R. Tan, E. Li, Antitumor effects of naturally occurring oligomeric resveratrol derivatives, *FASEB J* 27(11) (2013) 4561-71.
34. W. Zain, N. Ahmat, N. Norizan, N. Nazri, The evaluation of antioxidant, antibacterial and structural identification activity of trimer resveratrol from Malaysia's diptero-carpaceae, *J Basic Appl Sci* (2011) 926 - 929.
35. N. Mizushima, M. Komatsu, Autophagy: renovation of cells and tissues, *Cell* 147(4) (2011) 728-41.
36. S. Qin, G. Wang, L. Chen, H. Geng, Y. Zheng, C. Xia, S. Wu, J. Yao, L. Deng, Pharmacological vitamin C inhibits mTOR signaling and tumor growth by degrading Rictor and inducing HMOX1 expression, *Plos Genet* 19(2) (2023) e1010629.
37. D.D. Sarbassov, S.M. Ali, D.H. Kim, D.A. Guertin, R.R. Latek, H. Erdjument-Bromage, P. Tempst, D.M. Sabatini, Rictor, a novel binding partner of mTOR, defines a rapamycin-insensitive and raptor-independent pathway that regulates the cytoskeleton, *Curr Biol* 14(14) (2004) 1296-302.
38. M. Welcker, B. Clurman, FBW7 ubiquitin ligase: a tumour suppressor at the crossroads of cell division, growth and differentiation, *Nat Rev Cancer* 8(2) (2008) 83-93.
39. Y. Xu, X. Yang, Autophagy and pluripotency: self-eating your way to eternal youth, *Trends Cell Biol* 32(10) (2022) 868-882.
40. H. Yamamoto, S. Zhang, N. Mizushima, Autophagy genes in biology and disease, *Nat Rev Genet* (2023) 1-19.
41. H. Yang, J.X. Tan, Lysosomal quality control: molecular mechanisms and therapeutic implications, *Trends Cell Biol* (2023).
42. B.R. Stockwell, Ferroptosis turns 10: Emerging mechanisms, physiological functions, and therapeutic applications, *Cell* 185(14) (2022) 2401-2421.
43. H. Sung, J. Ferlay, R. Siegel, M. Laversanne, I. Soerjomataram, A. Jemal, F. Bray, Global cancer statistics 2020: GLOBOCAN estimates of incidence and mortality worldwide for 36 cancers in 185 countries, *CA Cancer J Clin* 71(3) (2021) 209-249.
44. Y. Li, J. Duan, X. Bian, S. Yu, Triple-negative breast cancer molecular subtyping and treatment progress, *Breast Cancer Res* 22 (1) (2020).
45. R. Shams, Y. Ito, H. Miyatake, Mapping of mTOR drug targets: Featured platforms for anti-cancer drug discovery, *Pharmacol Ther* 232 (2022) 108012.

## Author Contributions

Shiyang Lou: Conceptualization, Methodology, Writing—original draft, Investigation. Ruixu Zhang: Methodology, Writing—original draft, Investigation. Chao Xia: Methodology, Writing—original draft, Investigation. Yining Zheng: Methodology, Investigation. Miaomiao Zhu: Methodology, Investigation. Dingping Feng: Methodology, Investigation. Lu Deng: Conceptualization, Methodology, Writing—original draft, Investigation, Writing—review and editing, Resources, Supervision, Project administration and Funding acquisition.

## Funding information

The authors gratefully thank professor Pu Liu (Henan University of Science and Technology) for the help of compounds isolation and the members of the professor Junhu Yao lab for their assistance. This work was financially supported by the Shenzhen Municipal Basic Research Program (Natural Science Foundation) General Program Project (Grant No. JCYJ20240813152007010); National Natural Science Foundation of China - General Program Project (Grant No. 82472705).

## Conflict of interest statement

The authors declare that they have no conflict of interest.

## Data Availability Statement

The data that support the findings of this study are available from the corresponding author upon reasonable request.

## Ethical statement

We promise that the results of this study will be reported in an honest, objective, and responsible manner without any modification or manipulation that may mislead the reader or compromise the integrity of the study.

## SUPPORTING MATERIALS

Additional supplementary information is available for download and review in the supplementary information section located on the right-hand side of this article's HTML page.

**Supplementary+Data.pptx: Figure S1 - Figure S3**